Skewed, exponential pressure distributions from Gaussian velocities

Mark Holzer and Eric Siggia
Laboratory of Atomic and Solid State Physics, Cornell University, Ithaca, New York 14853-2501

(Received 17 February 1993; accepted 18 June 1993)

A simple analytical argument is given to show that the distribution function of the pressure and that of its gradient have exponential tails when the velocity is Gaussian. A calculation of moments implies a negative skewness for the pressure. Explicit analytical results are given for the case of the velocity being restricted to a shell in wave number. Numerical pressure distributions are presented for Gaussian velocities with realistic spectra. For real turbulent flows, one expects that the pressure distribution should retain exponential tails while the pressure gradients should develop stretched-exponential distributions. In the context of the theory, available numerical and laboratory data are examined for the pressure, along with data for the wall shear stress in a boundary layer.

I. INTRODUCTION

In an incompressible (unit density) flow, the pressure, p, is an instantaneous functional of the velocity, v_i, determined by

$$\nabla^2 p = -(\partial_i v_j)(\partial_j v_i) = \tfrac{1}{2}\omega^2 - s^2, \tag{1}$$

where repeated indices are summed, ω is the vorticity, and $s_{ij} = (\partial_i v_j + \partial_j v_i)/2$ is the rate-of-strain tensor. In spite of the appearance of the velocity gradients, standard arguments[1,2] imply that various scales contribute to the pressure an amount proportional to their kinetic energy, and hence the large scales dominate.[3]

The probability density function (pdf) of the pressure, in contrast to that of the pressure gradient, need not be symmetric, and, in fact, numerical simulations[4–6] and laboratory experiments[7] show that the pressure pdf is skewed to negative values, where it has an exponential tail. For isotropic turbulence, numerical simulations[5,6] show a less pronounced exponential tail for positive values. While the second equality in (1) suggests that intermittency-enhanced vorticity fluctuations could be responsible for the skewness,[4] the dominance of the pressure by the large scales argues otherwise. Indeed, Kimura and Kraichnan[8] have shown numerically that a Gaussian random velocity field generates a pressure field with negative skewness and exponential tails!

In this paper we show analytically that, for a Gaussian velocity, the pressure pdf has exponential tails and negative skewness in both two and three dimensions. Two dimensions is actually very relevant, because the energy-containing eddies of the Taylor–Green[9] simulations of Ref. 4, and those near walls, where the pressure was measured experimentally,[7] are not isotropic. Also, the skewness is generally larger in two than in three dimensions.

Merely the quadratic dependence of the pressure on the velocity can account for the exponential tails, and their occurrence is not an argument for "intermittency" under any reasonable definition of the term. In fact, we can conclude that the ability to fit the pdf for negative fluctuations by a single exponential for real turbulence data argues strongly that there is no information about intermittency or small scales encoded in the tail of the pdf. The large-scale velocity modes, which manifestly set the variance and skewness of the pressure, already yield an exponential, which, *provided it fits the data for all negative pressure fluctuations*, $p - \langle p\rangle \lesssim -\sqrt{\langle (p-\langle p\rangle)^2\rangle}$, leaves nothing to be explained by "intermittency."

Only a stretched exponential pdf, such as would be obtained from a sum of exponentially distributed quantities with decreasing amplitude and increasing variance, would be suggestive of small-scale contributions. Simulations[10] show something of this sort for pressure-gradient pdf's. Standard arguments[1] determine the variance of the pressure gradient, or Lagrangian acceleration, to be $\sim[\int_0^\infty kE(k)dk]^2$, where $E(k)$ is the usual energy spectrum. This expression is clearly dominated by small scales in the vicinity of the viscous cutoff. A purely Gaussian velocity, however, gives exponential tails not only for the pressure, but also for the pressure-gradient pdf.

In the following three sections we consider a Gaussian velocity field. We derive general bounds on the pressure and pressure-gradient pdf's, give several explicit analytical results, and present numerical pressure pdf's for a few interesting cases. In the conclusion, we return to the question of what to expect for the pdf's of the pressure and its gradient for real turbulent flows. We also examine available data for the pressure and speculate on the relevance of our theory to data for the wall shear stress from a turbulent boundary layer.

II. THE ANALYTIC STRUCTURE OF THE GENERATING FUNCTIONS

If $P(p)$ denotes the pdf of p, the generating function of $P(p)$, $\hat{P}_p(z) \equiv \int dp\, P(p)\exp(izp)$, is given by

$$\hat{P}_p(z) = \langle e^{izp(\mathbf{0})}\rangle_{\mathbf{v}}, \tag{2}$$

where the brackets denote an average over the velocity ensemble of interest. The asymptotic behavior of the pdf is determined by the analytic structure of its generating function according to standard results on Fourier transforms. (Because we are interested in a homogeneous system, we concentrate, for convenience, on the pdf of the pressure at

 0899-8213/93/5(10)/2525/8/$6.00

the origin, $p(\mathbf{x}=\mathbf{0})$ and assume periodic boundary conditions.) In terms of the Fourier transform of the velocity, $\mathbf{v}(\mathbf{k})=\int d\mathbf{x}\,\mathbf{v}(\mathbf{x})\exp(i\mathbf{x}\cdot\mathbf{k})$, the pressure becomes

$$p(\mathbf{0})=-\int (d\mathbf{k})(d\mathbf{q})\,\frac{k_i q_j v_i^*(\mathbf{q})v_j(\mathbf{k})}{(\mathbf{k}-\mathbf{q})^2}, \tag{3}$$

where the notation $(d\mathbf{k})$ means $d\mathbf{k}/(2\pi)^d$, $*$ denotes complex conjugation, and by virtue of $v_i^*(\mathbf{k})=v_i(-\mathbf{k})$, only half of the $v_i(\mathbf{k})$ are independent. In addition, we need to impose incompressibility, which is most easily done by expressing the velocity as the curl of a vector potential, $\mathbf{v}=\nabla\times\mathbf{A}$. In two dimensions, $\mathbf{A}=\hat{\mathbf{z}}\psi$, where the z axis is taken as normal to the two-dimensional plane and ψ is the familiar streamfunction. In terms of $\mathbf{A}$, the pressure becomes

$$p(\mathbf{0})=-\int (d\mathbf{k})(d\mathbf{q})\,\frac{\mathbf{A}^*(\mathbf{q})\cdot(\mathbf{k}\times\mathbf{q})(\mathbf{k}\times\mathbf{q})\cdot\mathbf{A}(\mathbf{k})}{(\mathbf{k}-\mathbf{q})^2}. \tag{4}$$

We will now assume the velocity field (and therefore the vector potential) to be Gaussian. The generating function for the pressure pdf thus becomes the functional integral,

$$\hat{P}_p(z)=\mathcal{N}\int \mathcal{D}\mathbf{A}(\mathbf{k})\delta[\mathbf{k}\cdot\mathbf{A}(\mathbf{k})]\exp\Bigg(-\int (d\mathbf{k})(d\mathbf{q}) \times[izM_{ij}(\mathbf{k},\mathbf{q})+(2\pi)^d\delta(\mathbf{k}-\mathbf{q})\delta_{ij}] \times\frac{kqA_i^*(\mathbf{k})A_j(\mathbf{q})}{\sigma(q)\sigma(k)}\Bigg), \tag{5}$$

where $\sigma^2(k)\equiv\langle\mathbf{v}^*(\mathbf{k})\cdot\mathbf{v}(\mathbf{k})\rangle$, $\mathcal{N}$ is a normalizing constant into which the purely numerical Jacobian, $|\delta\mathbf{v}/\delta\mathbf{A}|$, has been absorbed, and the (infinite-dimensional) matrix $\mathbf{M}$ is given by

$$M_{ij}(\mathbf{k},\mathbf{q})=\frac{\sigma(k)\sigma(q)}{kq}\,\frac{(\mathbf{k}\times\mathbf{q})_i(\mathbf{k}\times\mathbf{q})_j}{(\mathbf{k}-\mathbf{q})^2}. \tag{6}$$

The delta function in (5) constrains the vector potential to be transverse to ensure one-to-one correspondence between the fields $\mathbf{A}$ and $\mathbf{v}$. However, because $A_i^*M_{ij}A_j$ involves only the transverse part of $\mathbf{A}$, omitting the constraint, $\delta[\mathbf{k}\cdot\mathbf{A}(\mathbf{k})]$, introduces only a z-independent overall constant, which the normalization, $\hat{P}(z=0)=1$, eliminates.

The unrestricted, normalized Gaussian functional integral (5) evaluates to

$$\hat{P}(z)=\frac{1}{\sqrt{\mathrm{Det}(\mathbf{1}+iz\mathbf{M})}}. \tag{7}$$

Thus, singularities occur when i/z is an eigenvalue of $\mathbf{M}$, which puts them on the imaginary z axis because $\mathbf{M}$ is real and symmetric. Since $\mathbf{M}$ acts on a space of complex functions, its eigenfunctions are generally complex (eigenvalue λ_n), with the exception of those that are radial, i.e., a function of $|\mathbf{k}|$ only (eigenvalue λ_r), and hence purely real. Because the functional integral (5) involves separate integrals over the real and imaginary parts of each independent eigenfunction, it follows that (7) generally takes the form

$$\hat{P}(z)=\frac{1}{\Pi_r\sqrt{1+iz\lambda_r}\Pi_n(1+iz\lambda_n)}. \tag{8}$$

We will now show that the eigenvalues of $\mathbf{M}$ are bounded from above in absolute value by a finite number, λ, which means that poles cannot be closer to the real axis than $1/\lambda$. This, in turn, implies that the dominant asymptotic behavior of $P(p)$ is exponential, i.e., $P(p)\sim\exp(-|p/\lambda|)$ for large $|p|$, unless special circumstances remove all singularities from the upper or lower half of the z plane (we will show below that this occurs for pressure in two dimensions when the velocity lies on a shell in $\mathbf{k}$ space). To bound the eigenvalues of $\mathbf{M}$, choose an *arbitrary* vector, $\Psi(\mathbf{k})$, with adjoint $\Psi^\dagger(\mathbf{k})$, and form the quantity

$$\Lambda\equiv\frac{\Psi^\dagger\cdot\mathbf{M}\cdot\Psi}{\Psi^\dagger\cdot\Psi}\equiv\Bigg[\int (d\mathbf{k})(d\mathbf{q})\sigma(k)\sigma(q)\Psi^\dagger(\mathbf{k})\cdot\hat{\mathbf{n}}\hat{\mathbf{n}}\cdot\Psi(\mathbf{q}) \times\left(\frac{\sin^2\theta}{r-2\cos\theta}\right)\Bigg]\Bigg/\int (d\mathbf{k})|\Psi(\mathbf{k})|^2, \tag{9}$$

where $\hat{\mathbf{n}}$ is a unit vector along $\mathbf{k}\times\mathbf{q}$, $r\equiv k/q+q/k$, $\cos\theta=\mathbf{k}\cdot\mathbf{q}/(kq)$, and $|\Psi(\mathbf{k})|\equiv[\Psi_i^*(\mathbf{k})\Psi_i(\mathbf{k})]^{1/2}$. Since Ψ is arbitrary, a bound for $|\Lambda|$ is also clearly a bound for λ since, in particular, the bound must hold for Ψ being the eigenvector having the largest eigenvalue in absolute value. To bound $|\Lambda|$, we replace $\Psi\cdot\mathbf{n}$ with $|\Psi|$ and observe that $\sin^2\theta/(r-2\cos\theta)\leqslant 1$ for $r\geqslant 2$. Therefore

$$\lambda=\max|\Lambda| \leqslant\frac{(\int d\mathbf{k}\,\sigma|\Psi|)^2}{\int d\mathbf{k}|\Psi|^2}\leqslant\int d\mathbf{k}\,\sigma^2(k)=\langle|\mathbf{v}(\mathbf{x}=\mathbf{0})|^2\rangle, \tag{10}$$

the last inequality just being the Cauchy–Schwartz inequality. The bound in Eq. (10) agrees with conventional estimates[1] of $\sqrt{\langle(p-\langle p\rangle)^2\rangle}$.

The pdf of pressure gradients is also of some interest. The generating function of the pressure gradient in the x direction, say, $\partial_x p$, is simply obtained by replacing $\mathbf{M}$ in Eq. (5) and (7) by

$$M'_{ij}(\mathbf{k},\mathbf{q})=-i[(\mathbf{k}-\mathbf{q})\cdot\hat{\mathbf{x}}]M_{ij}(\mathbf{k},\mathbf{q}). \tag{11}$$

Since $\mathbf{M}'$ is Hermitian with respect to the continuous indices $\mathbf{k}$ and $\mathbf{q}$, and symmetric with respect to the discrete indices i and j, its eigenvalues are purely real placing the singularities again on the imaginary z axis. Furthermore, since the elements of $\mathbf{M}'$ are purely imaginary, the eigenvalues of $\mathbf{M}'$ must come in pairs $\pm\mu$, making the corresponding generating function a function of z^2 only. Thus, the pressure-gradient pdf is symmetric, i.e., invariant under

$\partial_x p \to -\partial_x p$. Physically this is, of course, unavoidable, as an isotropic fluid cannot preferentially accelerate in any particular direction.

To find a bound, λ', for the magnitude of the eigenvalues of $\mathbf{M}'$, we repeat the steps that led to the estimate for λ, except that we now use distinct right and left trial vectors, $\Psi_L(\mathbf{k})$ and $\Psi_R(\mathbf{q})$. The norm of the new factor, $(\mathbf{k}-\mathbf{q})\cdot\hat{\mathbf{x}}$, is bounded by $\sqrt{qk}\sqrt{r-2\cos\theta}$, and hence we can use the inequality $\sin^2\theta/\sqrt{r-2\cos\theta} \leqslant 1$ to eliminate all r dependence. Thus we derive

$$\lambda' \leqslant \Psi_L^\dagger \cdot \mathbf{M}' \cdot \Psi_R / (\Psi_L^\dagger \cdot \Psi_L \Psi_R^\dagger \cdot \Psi_R)^{1/2} \leqslant \int (d\mathbf{k}) k\sigma^2(k). \tag{12}$$

Note that if we assume a Kolmogorov spectrum for $k^{d-1}\sigma^2(k)$ with wave number cutoff η, then $\lambda' \sim \langle v^2\rangle L^{-2/3}\eta^{1/3}$, which scales like $\nu^{-1/4}$, where L is the integral scale and ν, the kinematic viscosity. This again agrees with conventional estimates[1] for $\sqrt{\langle(\partial_x p)^2\rangle}$.

It is very interesting to note that both $\mathbf{M}^2$ and $\mathbf{M}'^2$ have a trace of order the square of the eigenvalue bounds just derived, e.g.,

$$\mathrm{Tr}(\mathbf{M}^2) = \int (d\mathbf{k})(d\mathbf{q})\sigma^2(k)\sigma^2(q)\left(\frac{\sin^2\theta}{r-2\cos\theta}\right)^2 \leqslant \langle|\mathbf{v}(\mathbf{0})|^2\rangle^2. \tag{13}$$

Because there is no factor of order the dimensionality of the space on which $\mathbf{M}$ or $\mathbf{M}'$ acts, which is infinite in the continuum limit, their eigenvalues are square summable and can only accumulate at zero. In other words, there must be gaps between all nonzero eigenvalues, particularly between the largest, and all the others. In the extreme case of two dimensions and the velocity restricted to a shell in k space, all but two of the eigenvalues are identically zero (cf. the Appendix). Because the leading singularity is isolated, one sees by deforming the integration contour for the pdf that the form of the tails can be calculated exactly. Thus, if the leading singularity has a square root [cf. Eq. (8)], $P(p) \propto |p|^{-1/2}\exp[\pm(\text{const})p]$, while a simple pole just gives $P(p) \propto \exp[\pm(\text{const})p]$. Our concluding discussion as to the form of the pdf for a realistic velocity ensemble will also exploit the discrete spectrum of $\mathbf{M}$.

III. EXPLICIT ANALYTICAL RESULTS

Having established the exponential tails of the pressure pdf, we now compute its skewness by taking moments of Eq. (4). Since we are assuming the velocity field to be Gaussian, averages of products of $2n$ velocities simply decompose into products of n averages of two velocities, $\langle vv\rangle$, paired in all possible ways. Because of isotropy, homogeneity, and incompressibility the $\langle vv\rangle$ averages must take the form

$$\langle v_i(\mathbf{k})v_j(\mathbf{q})\rangle = (2\pi)^d\delta(\mathbf{k}+\mathbf{q})\left(\delta_{ij}-\frac{k_ik_j}{k^2}\right)f(k), \tag{14}$$

with $f(k)$ defined by

$$f(k) \equiv \frac{(2\pi)^d}{(d-1)}\frac{2E(k)}{C_d k^{d-1}}, \tag{15}$$

where $E(k)$ is the spectrum of the turbulence, defined by $\langle \mathbf{v}(\mathbf{x})\cdot\mathbf{v}(\mathbf{x})\rangle/2 = \int_0^\infty E(k)dk$, and $C_d = 2(\pi)^{d/2}/\Gamma(d/2)$ is the surface area of a unit sphere in d dimensions.

After some algebra, we find

$$\langle p^2\rangle_c = 2\int (d\mathbf{k}_1)(d\mathbf{k}_2)f(k_1)f(k_2)k_1^2k_2^2\frac{(\hat{\mathbf{k}}_1\times\hat{\mathbf{k}}_2)^4}{(\mathbf{k}_1-\mathbf{k}_2)^4}, \tag{16}$$

and

$$\langle p^3\rangle_c = -8\int (d\mathbf{k}_1)(d\mathbf{k}_2)(d\mathbf{k}_3)f(k_1)f(k_2)f(k_3)k_1^2k_2^2k_3^2 \times\frac{(\hat{\mathbf{k}}_1\times\hat{\mathbf{k}}_3)\cdot(\hat{\mathbf{k}}_3\times\hat{\mathbf{k}}_2)}{(\mathbf{k}_1-\mathbf{k}_2)^2}\frac{(\hat{\mathbf{k}}_2\times\hat{\mathbf{k}}_1)\cdot(\hat{\mathbf{k}}_1\times\hat{\mathbf{k}}_3)}{(\mathbf{k}_2-\mathbf{k}_3)^2} \times\frac{(\hat{\mathbf{k}}_3\times\hat{\mathbf{k}}_2)\cdot(\hat{\mathbf{k}}_2\times\hat{\mathbf{k}}_1)}{(\mathbf{k}_3-\mathbf{k}_1)^2}, \tag{17}$$

where $\langle X^n\rangle_c \equiv \langle (X-\langle X\rangle)^n\rangle$. In two dimensions, the integrand of (17) can be expressed as

$$f(k_1)f(k_2)f(k_3)k_1^2k_2^2k_3^2\frac{\sin^2(\theta_{12})}{(\mathbf{k}_1-\mathbf{k}_2)^2}\frac{\sin^2(\theta_{23})}{(\mathbf{k}_2-\mathbf{k}_3)^2}\frac{\sin^2(\theta_{31})}{(\mathbf{k}_3-\mathbf{k}_1)^2}, \tag{18}$$

which is positive definite giving a negative definite skewness in two dimensions, independent of the spectrum. In three dimensions, the sign of the skewness is not immediately evident, since the cross products of (17) are not always aligned in three dimensions.

We now consider the special case of purely on-shell modes, $f(k) = (2\pi)^d\delta(k-k_0)f_0$, which allows explicit evaluation of the moments. We find

$$\langle p^2\rangle_c = \begin{cases} 3\pi^2k_0^2f_0^2, & \text{if } d=2, \\ \frac{32}{3}\pi^2k_0^4f_0^2, & \text{if } d=3, \end{cases} \tag{19}$$

and

$$\langle p^3\rangle_c = \begin{cases} -10\pi^3k_0^3f_0^3, & \text{if } d=2, \\ -\frac{224}{9}\pi^3k_0^6f_0^3, & \text{if } d=3. \end{cases} \tag{20}$$

Thus we obtain for the skewness, $S \equiv \langle p^3\rangle_c/\langle p^2\rangle_c^{3/2}$,

$$S = \begin{cases} -\frac{10}{3^{3/2}} = -1.924\,50..., & \text{if } d=2, \\ -\frac{7}{4\sqrt{6}} = -0.714\,43..., & \text{if } d=3. \end{cases} \tag{21}$$

For the case of on-shell velocity in two dimensions, the generating function for both the pressure and pressure gradient can easily be evaluated explicitly (for details, see the Appendix). If $P_N(X)$ denotes the pdf of X scaled to unit variance, and $\hat{P}_{X_N}(z)$ the corresponding generating function, we find

$$\hat{P}_{p_N}(\sqrt{3}z) = \frac{1}{(1+iz)\sqrt{1+2iz}}, \tag{22}$$

for the generating function of the pressure and

$$\hat{P}_{\partial_x p_N}(2z)=\frac{1}{\sqrt{(1+z^2)(1+3z^2)}}, \tag{23}$$

for the generating function of the pressure gradient. Note that (22) implies that $P_N(p)$ is identically zero for $p \geqslant 0$, i.e., for $p-\langle p\rangle \geqslant (2/\sqrt{3})\sqrt{\langle p^2\rangle_c}$, since all the singularities lie in the upper half of the z plane. The pressure-gradient pdf is symmetric, as expected. From the explicit generating functions the moments of the corresponding pdf's are easily computed by differentiating

$$\langle X^n\rangle=(-i)^n\left(\frac{\partial^n}{\partial z^n}\hat{P}_X(z)\right)_{z=0}. \tag{24}$$

The pressure pdf is the inverse Fourier transform of (22), which, for $p<0$, may be expressed in terms of the degenerate hypergeometric[11] function ${}_1F_1(\beta,\gamma,\xi)$ as

$$P_N\left(\frac{p}{\sqrt{3}}\right)=\sqrt{\frac{6}{\pi}}e^p\sqrt{-p}\,{}_1F_1\left(\frac{1}{2},\frac{3}{2},-\frac{p}{2}\right). \tag{25}$$

The pdf's have the following asymptotic forms: For p large and negative,

$$P_N\left(\frac{p}{\sqrt{3}}\right)=\sqrt{\frac{3}{\pi}}\frac{e^{p/2}}{\sqrt{-p/2}}\left[1+\mathcal{O}\left(\frac{1}{p}\right)\right], \tag{26}$$

and for large $|\partial_x p|$,

$$P_N\left(\frac{\partial_x p}{2}\right)=\frac{1}{\sqrt{\pi}}\frac{e^{-|\partial_x p|/\sqrt{3}}}{\sqrt{|\partial_x p|/\sqrt{3}}}\left[1+\mathcal{O}\left(\frac{1}{p}\right)\right]. \tag{27}$$

IV. PRESSURE pdf's FOR REALISTIC SPECTRA

We computed the pressure pdf numerically in three dimensions on a 112^3, and in two dimensions on a 256^2 lattice, with units chosen to make the minimum wave number unity. All convolutions were fully dealiased using the algorithm of Ref. 12, and many realizations of the Gaussian velocity were averaged to improve the statistics.

In two dimensions we considered a velocity having an equilibrium spectrum[13] $E(k)\propto k/(k_0^2+k^2)$. Figure 1 shows the resulting pressure pdf ($k_0=6$ and $k<118$), together with the exact on-shell result of Eq. (25). Note that the pdf for the equilibrium spectrum, as for any generic spectrum, has an exponential tail for $p-\langle p\rangle>0$, unlike the extreme on-shell case. The pdf for the equilibrium spectrum is characterized by a skewness of $S=-1.1885\pm0.0005$ and a kurtosis $K\equiv\langle(p-\langle p\rangle)^4\rangle/\langle p^2\rangle_c^2=6.44\pm0.01$. When the velocity is restricted to a shell, $S=-1.924\,50...$ and $K=9$ [cf. Eq. (22)].

With a $k^{-5/3}$ Kolomogorov spectrum in three dimensions, we obtain the pressure pdf of Fig. 2, which has $S=-0.490\pm0.002$ and $K=4.21\pm0.05$. We also verified that the pressure spectrum is proportional to $k^{-7/3}$, in agreement with the scaling arguments of Ref. 1. When the velocity is restricted to a "shell" in three dimensions ($24\leqslant k\leqslant 25$), the pdf has $S=-0.7132\pm0.0001$ and $K=4.34\pm0.01$ (also shown in Fig. 2). This skewness agrees with the result for a δ-function shell, Eq. (21), to 0.2%, and is the largest we found in three dimensions for any spectrum. Note that in three dimensions, even the shell case has an exponential tail for $p-\langle p\rangle>0$.[14]

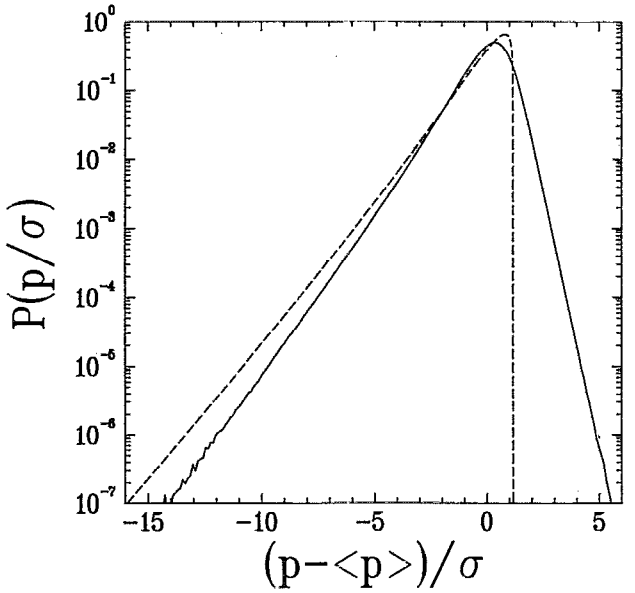

FIG. 1. Pressure pdf's in two dimensions; $\sigma\equiv\sqrt{\langle p^2\rangle_c}$. Solid line: The numerical pdf for $E(k)\sim k/(k_0^2+k^2)$, with $k_0=6$ and $k<118$, obtained from 10^4 independent realizations of the velocity field on a 512^2 lattice. $S=-1.1885\pm0.0005$ and $K=6.44\pm0.01$. Dashed line: The exact result for on-shell velocity. The absence of an exponential tail for positive p is particular to the on-shell velocity in two dimensions.

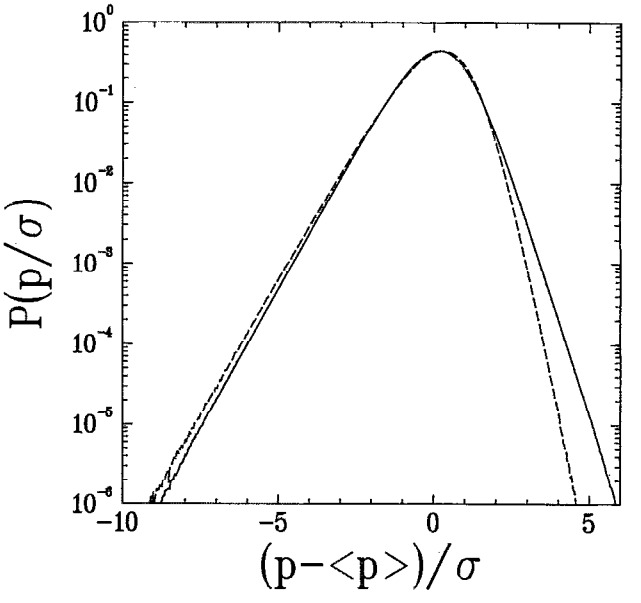

FIG. 2. Numerical pdf's for pressure in three dimensions on a 112^3 lattice; $\sigma\equiv\sqrt{\langle p^2\rangle_c}$. Solid line: $k^{-5/3}$ Kolmogorov spectrum, 10^4 independent realizations of the velocity field. Here $S=-0.490\pm0.002$ and $K=4.21\pm0.05$. Dashed line: On-shell velocity ($24\leqslant k\leqslant 25$), 10^3 independent realizations of the velocity field. Here $S=-0.7132\pm0.0001$ and $K=4.34\pm0.01$. Note that unlike in two dimensions, the 3-D on-shell case has an exponential tail for $p-\langle p\rangle>0$.

IV. CONCLUSIONS

What can we say about the pressure pdf of real flows based on our treatment for Gaussian velocities? Throughout this discussion, we use Galilean invariance to refer to the velocity relative to that at $\mathbf{r}=\mathbf{0}$, where the pressure is measured. To make this explicit, we use the notation $\Delta\mathbf{v}(\mathbf{r})\equiv\mathbf{v}(\mathbf{r})-\mathbf{v}(\mathbf{0})$. The distribution, $\rho(\Delta\mathbf{v})$, of an arbitrary velocity ensemble depends, *a priori*, on the *entire* field $\Delta\mathbf{v}$. Let us use the eigenvectors of the pressure matrix, $\mathbf{M}$, as a basis for the velocity field. We should then be able to limit consideration to only those modes for which $\Delta\mathbf{v}$ has appreciable variance, i.e., to those corresponding to the energy-containing scales. Since $\mathbf{M}$ has a discrete spectrum, it should, therefore, suffice to consider a finite number of modes. If we assume on experimental grounds[1,15,16] that for all such modes $\rho\to\exp[-\text{const}(\Delta v)^{\alpha}]$, with $\alpha\equiv 2$, as $|\Delta v|\to\infty$, then again we find that $\hat{P}(z)$ has a strip of analyticity. [If α were larger than 2, $\hat{P}(z)$ would be entire, while $\alpha<2$ would put singularities on the real axis.] Whether the leading singularity of $\hat{P}(z)$ is a square root or not depends on whether the corresponding eigenstate has spherical symmetry in $\mathbf{k}$ space, and on the precise way in which $\rho(\Delta v)$ limits to its asymptotic form.

It is interesting to note that a skewness of Δv can easily be accommodated[15] by assuming $\rho(\Delta v)\sim\exp[-(\Delta v)^2 f(\Delta v)]$, where $f(\Delta v)$ is a positive, monotonically increasing function that tends to a constant as $\Delta v\to\pm\infty$. When we introduce a skewness in this way, but keep the variance fixed, the tails of $P(p)$ move up (the leading singularities move closer to the real axis) because the integral on Δv diverges as $\Delta v\to-\infty$ for smaller $|\operatorname{Im} z|$ than it otherwise would. Something like this effect was observed by Kimura and Kraichnan.[8]

It follows from the preceding discussion that experimental pdf's should be represented by a generating function that has a strip of analyticity. A reasonable ansatz is

$$\hat{P}(z)=\frac{1}{\sqrt{1+i\lambda_0 z}\,\Pi_n(1+i\lambda_n z)}, \tag{28}$$

where the λ_n are, for simplicity, taken to be real, and $|\lambda_n|\to 0$ as $n\to\infty$. Inclusion of an infinite number of λ_n guarantees that $P(p)$ is infinitely differentiable at the origin, although fits to experimental data do not require such precision. Clearly, there are enough parameters in (28) to fit nearly anything, so that data analysis is only illuminating to the extent that it is reasonably successful with only a few parameters, as we shall now demonstrate.

We nondimensionalize all pdf's by scaling to unit variance and shifting to zero mean (the zero of pressure is arbitrary). Figure 3 shows the pdf for wall pressure measurements compared with the Kolmogorov curve of Fig. 2, and a two-parameter fit with the form (28), taking[17] $\Pi_n(1+i\lambda_n z)=\Pi_{n=1}^{\infty}[1+i\lambda_0 z/(an)][1-i\lambda_0 z/(bn)]$ (λ_0 is a uniform scale on z). The fit is excellent for $p-\langle p\rangle<0$, but poor in the tail for $p-\langle p\rangle>0$, where the data may be fitted to $(p-p_0)$,[4] as noted in Ref. 7. If taken literally, one would infer that the corresponding $\hat{P}(z)$ is analytic for $\operatorname{Im} z<0$, and that the first singularity for $\operatorname{Im} z>0$ is a fifth-order pole. Needless to say, this appears nongeneric, and we can only speculate that the rather large transducers used in the experiment might have biased the measurements. Although Ref. 7 provides some evidence that the transducer was sufficiently small to give effectively a point measurement, it is very hard to see on theoretical grounds why $\hat{P}(z)$ should be analytic for $\operatorname{Im} z<0$.

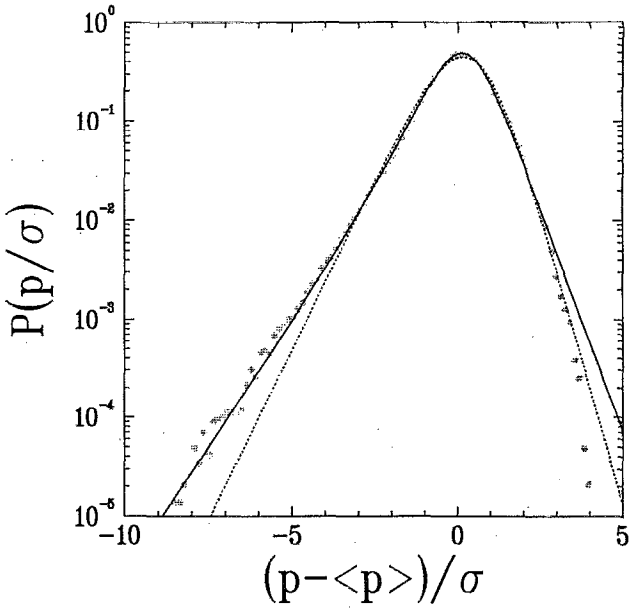

FIG. 3. A fit (solid line) to the wall-pressure data of Ref. 7 from the swirling flow between two parallel counter-rotating disks ($\Omega=1250$ rpm) using the generating function $\hat{P}(z)=(1+iz)^{-1/2}\times\Pi_{n=1}^{\infty}[1+iz/(an)]^{-1}[1-iz/(bn)]^{-1}$, with $a=2.5$ and $b=1.9$. The product was truncated at $n=50$. Also shown (dotted line) is the Kolmogorov curve of Fig. 2. Here $\sigma\equiv\sqrt{\langle p^2\rangle_c}$.

As shown in Fig. 4, we were more successful in fitting the pressure pdf from the statistically isotropic simulations of Ref. 6, using the same two-parameter form as for Fig. 3. The slight upward curvature of the tail of the fit for $p-\langle p\rangle<0$ is due to the leading singularity, having a square root [cf. Eq. (26)]. The fit is excellent down to $P(p)\sim 10^{-4}/\sqrt{\langle p^2\rangle_c}$, where the data veers off the fit. The pdf of Fig. 2 for the $k^{-5/3}$ spectrum fits the data less well than what is shown, presumably because of the skewness of the velocity.

Following our remarks in the Introduction, the difference between our exponential fit and the data in Fig. 4 represents events that could be attributable to intermittency. This view is reinforced by recent measurements,[18] which again have more weight in the far negative tail than an exponential fit to the center would allow. The experimenters are able to associate these large negative excursions with the intense vorticity tubes (diameter on the order of the dissipation scale) that they saw in their earlier visualizations.[19] This suggests that the far negative tail comes from small-scale events, which means that near dissipation-scale velocity differences of order several times $\sqrt{\langle|\mathbf{v}|^2\rangle}$ must be occurring. Recent simulations have indeed found velocity differences of this order in the imme-

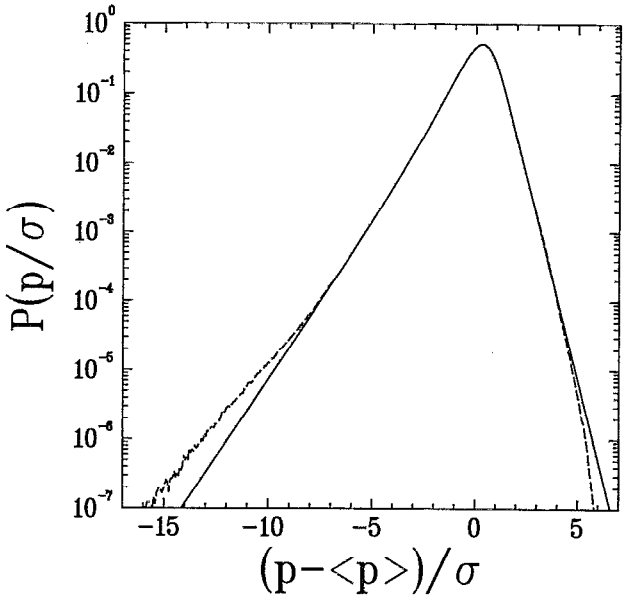

FIG. 4. A fit (solid line) to the pressure pdf for the isotropic simulations of Ref. 6 (dashed line) using $\hat{P}(z)=(1+iz)^{-1/2}\times\Pi_{n=1}^{\infty}[1+iz/(an)]^{-1}[1-iz/(bn)]^{-1}$, with $a=2.4$ and $b=1.75$. The product was truncated at $n=10$. $\sigma\equiv\sqrt{\langle p^2\rangle_c}$.

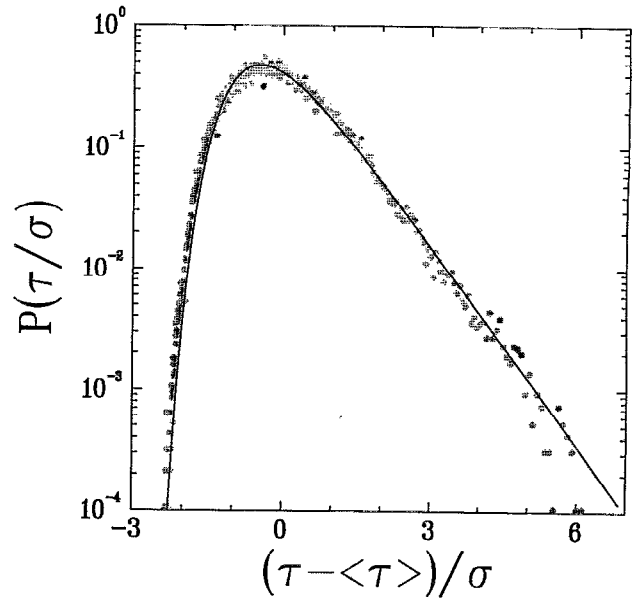

FIG. 5. The data for the wall shear stress, τ, of Ref. 21, fit with $\hat{P}(z)=\Pi_{n=1}^{\infty}(1-iz/n)^{-1}$. The product was truncated at $n=50$. Here $\sigma\equiv\sqrt{\langle\tau^2\rangle_c}$.

diate vicinity of vortex tubes.[20] This phenomenon is a severe violation of Kolmogorov scaling!

Pressure pdf's are also available from the Taylor–Green simulations of Ref. 4. These pdf's show more structure[4] (and probably have larger error bars) than the data in Fig. 4. For Reynolds numbers of Re=1600, 3000, and 5000, these pdf's have skewnesses of $S=-2.20$, -1.93, and -2.30, respectively, and are similar to our 2-D-shell Gaussian case ($S=-1.92$), with a pronounced tail for $p-\langle p\rangle<0$ and a sharp drop for $p-\langle p\rangle>0$.

We feel it is useful to speculate on the distribution of the wall shear stress of a turbulent boundary layer, since high quality data is available from Couette–Taylor flows,[21] and comparison with even the minimal theory of this paper does raise interesting testable predictions. Outside of the viscosity-dominated region near the wall, the momentum-flux tensor is a quadratic functional of the velocity analogous to the pressure. One can speculate that the near-wall region simply passively transmits the large-scale velocity fluctuations, which may dominate the fluctuations in the wall shear stress. Hence, we again employ Eq. (28), with all singularities restricted to $\mathrm{Im}\,z>0$, as required by the data. For simplicity, we omit the square-root singularity[22] and take $\lambda_n=-1/n$. The corresponding pdf has no adjustable parameters after shifting to zero mean and scaling to unit variance. At the very least, the quality of the fit of Fig. 5 shows that "intermittency" is not needed to explain the data.

Finally, we venture a few remarks about the pressure-gradient pdf for real flows. Our remarks are necessarily speculative because small-scale velocity differences dominate, and these are exponentially distributed.[23,16] Inverting the Laplacian of Eq. (1), and integrating once by parts (assuming periodic boundary conditions that eliminate surface terms), the pressure gradient is given by

$$\partial_i p(\mathbf{0})=\int d\mathbf{r}\,[\partial_i\partial_m G(\mathbf{r})]\,\Delta v_n\,\partial_n v_m, \tag{29}$$

where $\nabla^2 G(\mathbf{r})=-\delta(\mathbf{r})$, and again we use $\Delta\mathbf{v}\equiv\mathbf{v}(\mathbf{r})-\mathbf{v}(\mathbf{0})$. While (29) suggests a value of $\langle(\partial_x p)^2\rangle\sim\langle(\Delta\mathbf{v})^2\rangle\langle(\partial_x\mathbf{v})^2\rangle$, this is larger by a factor of $(L\eta)^{2/3}$ than the conventional estimate[1] noted in the Introduction. The latter is obtained via an additional integral by parts, which is legitimate since $|\Delta\mathbf{v}|\sim r$ for $r\ll 1/\eta$, so that the singularity at $r=0$ is integrable. We therefore use as an estimate for $\partial_x p$ what is in effect a bound obtained by suppressing indices:

$$\partial_x p\sim\int_0^{\sim L}\frac{(\Delta\mathbf{v})^2}{r^2}\,dr. \tag{30}$$

Clearly, the largest contribution to (30) comes from $r\sim 1/\eta$, because for larger r, $|\Delta\mathbf{v}|\sim r^{1/3}$ (e.g., Ref. 1). For the pressure itself, the corresponding integral, $p\sim\int_0^{\sim L}(\Delta v)^2 r^{-1}\,dr$, is dominated by the integral scale, L. Equation (30) implies that if $\Delta\mathbf{v}$ has an exponential pdf, then $\partial_x p$ is distributed like a stretched exponential, viz.,

$$P(\partial_x p)\sim e^{-(\mathrm{const})|\partial_x p|^{1/2}}, \tag{31}$$

in analogy with Ref. 24.

ACKNOWLEDGMENTS

M. Brachet, S. Fauve, M. Meneguzzi, H. Swinney, and P. Umbanhowar kindly provided their pdf data for us to fit. We thank them, together with O. Cadot, Y. Couder, R. Kraichnan, A. Pumir, and B. Shraiman for discussions.

Our research was supported by the Air Force Office of Scientific Research under Grant No. 91-0011, and by the National Science Foundation under Grant No. DMR 9012974. M.H. acknowledges support from the Cornell Materials Science Center and E.S. thanks the Courant Institute for their hospitality and support (AFOSR Grant No. 90-0090) during a visit.

APPENDIX: pdf's IN TWO DIMENSIONS FOR AN ON-SHELL VELOCITY

We denote the Fourier transform of the on-shell streamfunction by $\psi(\theta)=\psi^*(\theta+\pi)$, where θ is the direction of the wave vector (which lies on a circle; the "shell"). The pressure is then given by

$$p(\mathbf{0})=-c\int_0^{2\pi}\int_0^{2\pi} d\theta_1\, d\theta_2\, \psi^*(\theta_1) \times[1+\cos(\theta_1-\theta_2)]\psi(\theta_2). \tag{A1}$$

Since we will scale the pdf to unit variance at the end, we set the dimensional constant $c=1/(4\pi^2)$. Expression (A1) becomes diagonal by expressing $\psi(\theta)$ in terms of circular harmonics as

$$\psi(\theta)=\sum_{n=-\infty}^{\infty}\tilde{\psi}_n e^{in\theta}. \tag{A2}$$

The condition $\psi(\theta)=\psi^*(\theta+\pi)$ implies

$$\tilde{\psi}_n=(-1)^n\tilde{\psi}^*_{-n}. \tag{A3}$$

By homogeneity, $\langle\tilde{\psi}^*_n\tilde{\psi}_m\rangle \propto \delta_{n,m}$ and by isotropy all $\tilde{\psi}_n$ have the same variance, which we set to unity. Writing $\tilde{\psi}_n\equiv x_n+iy_n$, and noting that (A3) implies $y_0=0$, the generating function, Eq. (5), becomes

$$\hat{P}(z)=\mathcal{N}\int dx_0\, dx_1\, dy_1\, e^{-(iz+1/2)x_0^2-(iz+1)(x_1^2+y_1^2)} =\mathcal{N}\frac{\pi}{1+iz}\sqrt{\frac{2\pi}{1+2iz}}. \tag{A4}$$

Normalizing and scaling to unit variance produces Eq. (22).

The pressure gradient is given by

$$\partial_x p(\mathbf{0})=ic'\int_0^{2\pi}\int_0^{2\pi} d\theta_1\, d\theta_2\, \psi^*(\theta_1)[1+\cos(\theta_1-\theta_2)] \times[\cos(\theta_1)-\cos(\theta_2)]\psi(\theta_2). \tag{A5}$$

We expand $\psi(\theta)$ in circular harmonics and proceed as for the pressure pdf to obtain

$$\hat{P}(z)=\mathcal{N}\int dx_0\, dx_1\, dy_1\, dx_2\, dy_2\, e^{-\Psi_i B_{ij}\Psi_j}, \tag{A6}$$

where $\Psi\equiv(x_0,x_1,x_2,y_1,y_2)$ and

$$\mathbf{B}=\begin{pmatrix} 1/2 & 0 & 0 & -iz & 0 \\ 0 & 1 & 0 & 0 & -iz \\ 0 & 0 & 1 & iz & 0 \\ -iz & 0 & iz & 1 & 0 \\ 0 & -iz & 0 & 0 & 1 \end{pmatrix}. \tag{A7}$$

Normalizing and scaling to unit variance gives Eq. (23) as $\hat{P}_{\partial_x p_N}(2z) = [2\,\mathrm{Det}(\mathbf{B})]^{-1/2}$.

[1] A. S. Monin and A. M. Yaglom, *Statistical Fluid Mechanics* (MIT Press, Cambridge, MA, 1975), Vol. 2, pp. 368–377.
[2] M. Nelkin and M. Tabor, "Time correlations and random sweeping in isotropic turbulence," Phys. Fluids A **2**, 1 (1990).
[3] For measured pressure spectra and correlation functions beneath turbulent boundary layers, see W. W. Willmarth, "Pressure fluctuations beneath turbulent boundary layers," Annu. Rev. Fluid Mech. **7**, 13 (1975).
[4] M. E. Brachet, "Direct simulation of three-dimensional turbulence in the Taylor–Green vortex," Fluid Dyn. Res. **8**, 1 (1991).
[5] O. Métais and M. Lesieur, "Spectral large-eddy simulations of isotropic and stably stratified turbulence," J. Fluid Mech. **239**, 157 (1992).
[6] A. Vincent and M. Meneguzzi, "The spatial structure and statistical properties of homogeneous turbulence," J. Fluid Mech. **225**, 1 (1991); M. Meneguzzi (private communication).
[7] S. Fauve, C. Laroche, and B. Castaing, "Pressure fluctuations in swirling turbulent flows," J. Phys. II France **3**, 271 (1993).
[8] Y. Kimura and R. H. Kraichnan (private communication). They observed numerically that the pressure had exponential tails for a Gaussian-random initial velocity and that these tails lifted up, increasing the skewness, as the initial state was evolved under the dynamics. Also see R. H. Kraichnan, in *Nonlinear and Relativistic effects in Plasmas*, edited by V. Stefan (American Institute of Physics, New York, 1992).
[9] M. E. Brachet, D. I. Meiron, S. A. Orszag, B. G. Nickel, R. H. Morf, and U. Frisch, "Small-scale structure of the Taylor–Green vortex," J. Fluid Mech. **130**, 411 (1983).
[10] P. K. Yeung and S. B. Pope, "Lagrangian statistics from direct numerical simulations of isotropic turbulence," J. Fluid Mech. **207**, 531 (1989).
[11] The function ${}_1F_1(\beta,\gamma,\zeta)$ is also known as Kummer's function $M(\beta,\gamma,\zeta)$. Furthermore, $M(\frac{1}{2},\frac{3}{2},x)=-(\sqrt{\pi}/2)\mathrm{sign}(x)\mathrm{erf}(\sqrt{-x})/\sqrt{-x}$ so that Eq. (25) involves the error function of imaginary argument. See, e.g., M. Abramovitz and I. A. Stegan, *Handbook of Mathematical Functions* (Dover, New York, 1972), p. 504.
[12] G. S. Patterson and S. A. Orszag, "Spectral calculations of isotropic turbulence: Efficient removal of aliasing interactions," Phys. Fluids **14**, 2538 (1971).
[13] See, e.g., R. H. Kraichnan, "Inertial ranges in two-dimensional turbulence," Phys. Fluids **10**, 1417 (1967).
[14] The errors given here are sampling errors only. The moments of the pressure pdf are sensitive to modes in $v_i(\mathbf{r})v_j(\mathbf{r})$ that are not resolved. The associated resolution error is on the order of a few percent. For example, if we compute the pressure on a 64^3 lattice with the Kolmogorov spectrum, we find $S=-0.501\pm0.002$ and $K=4.22\pm0.08$. (Recomputing the pressure for the 2-D equilibrium spectrum on a 256^2 lattice, again with $k_0=6$ and $k<118$, we obtain $S=-1.1435\pm0.0005$ and $K=6.26\pm0.01$.)
[15] B. Castaing, Y. Gagne, and E. J. Hopfinger, "Velocity probability density functions of high-Reynolds number turbulence," Physica D **46**, 177 (1990).
[16] Y. Gagne, E. Hopfinger, and U. Frisch, in *New Trends in Nonlinear Dynamics and Pattern Forming Phenomena: The Geometry of Nonequilibrium*, Proceedings of a NATO Advanced Research Workshop, Cargèse, France, 1988, edited by P. Coullet and P. Huerre (Plenum, New York, 1990), p. 315.

[17]Note that with N terms in the product, this generating function leads to $\langle p\rangle = \frac{1}{2} + (1/a - 1/b)\Sigma_{n=1}^{N} 1/n$, which (for $a \neq b$) diverges like $\log N$ as $N \to \infty$. However, this is not a problem because for any finite N we can always shift the pdf so that $\langle p\rangle = 0$, and because $\langle (p - \langle p\rangle)^m\rangle$ for $m > 1$ converges like $(\text{const} + 1/N^{m-1})$. The rapid convergence of the higher moments allows truncation of the product at finite N.
[18]Y. Couder, O. Cadot, and S. Douady (private communication).
[19]S. Douady, Y. Couder, and M. E. Brachet, "Direct observation of the intermittency of intense vorticity filaments in turbulence," Phys. Rev. Lett. **67**, 983 (1991).
[20]J. Jimenez, A. Wray, P. Saffman, and R. Rogallo, "The structure of intense vorticity in isotropic turbulence," J. Fluid Mech (in press).
[21]D. P. Lathrop, J. Fineberg, and H. L. Swinney, "Transitions to shear-driven turbulence in Couette–Taylor flow," Phys. Rev. A **46**, 6390 (1992).
[22]This generating function again has a logarithmically diverging first moment with all higher moments converging (cf. Ref. 17). We also fitted the data to the zero-parameter form, $\hat{P}(z) = (1 - iz)^{-1/2} \times \Pi_{n=2}^{\infty}(1 - iz/n)^{-1}$ with slightly worse results.
[23]C. W. Van Atta and W. Y. Chen, "Structure functions of turbulence in the atmospheric boundary layer over the ocean," J. Fluid Mech. **44**, 145 (1970).
[24]R. H. Kraichnan, "Models of intermittency in hydrodynamic turbulence," Phys. Rev. Lett. **65**, 575 (1990).